ARTICLE NO. 79-0256R

A80-043

Two-Impulse Orbit Transfer Error Analysis via Covariance Matrix

40005
40016
10005

G. Porcelli*
International Telecommunication Satellite Organization, Washington, D.C.
and
E. Vogel†
Fairchild Space and Electronics Company, Germantown, Md.

An algorithm for the determination of the orbit insertion errors in two-impulse noncoplanar orbital transfers, with fixed time between the impulses, is presented. Inputs to the algorithm are the covariance matrices of the source errors, and the nominal parameters of the transfer. The results yield the covariance matrix of the post-orbit insertion errors, also expressed in terms of the final orbit element errors. The method requires that the second impulse be delivered at an apogee.

Nomenclature

a = semimajor axis
c = cosine
C = covariance matrix
e = eccentricity
E = eccentric anomaly
H = angular momentum
i = inclination
n = normal (transverse) displacement
p = semiparameter
r = orbit radius
s = sine
t = time
T = transfer matrix
V = velocity
α = plane change
β = path angle (measured from outward vertical)
γ = velocity azimuth
δ = angle between V and V_{motor}
Δ = increment or error
ζ = yaw error (positive with nose left)
λ = latitude
ξ = pitch error (positive with nose down)
τ = orbit period
ϕ = true anomaly
Ω = nodal position

Subscripts/Superscripts

a = apogee
f = post-orbit insertion
p = initial point of transfer orbit
N = normal
R = radial
T = tangential
t = matrix transpose
0 = initial condition
1 = apsidal
2 = transverse

Introduction

THIS paper describes an algorithm for closed-form estimation of orbit insertion errors in any single- or dual-impulse orbital transfer. Typically, the method applies to a mission model consisting of: 1) insertion into a transfer orbit, starting from a noncoplanar parking orbit, or from suborbital initial conditions, followed by 2) insertion, near transfer orbit apogee, into noncoplanar final orbit. The stage motors' ignition may be time scheduled or independently controlled.

The method assumes that statistical description of the initial condition errors and of the error contribution of each stage be available in the form of covariance matrices. The method consists of propagating these source errors throughout the subsequent transfer. Source errors introduced at intermediate stages of the transfer are treated as statistically independent of the existing cumulative errors, thus the covariance matrix of their effects is added to the corresponding matrix of the propagating errors. Alternately, the orbit insertion errors could be estimated by a Monte Carlo technique. The advantages of a closed-form approach are simplicity and smaller computation time.

The originality of this algorithm is not in the covariance matrix formulation, well known from estimation theory,[1,2] but in the derivation of the propagation (transfer) matrices. Some of these are obtained by simple geometrical considerations associated with the impulsive velocity vector composition, others are derived from Keplerian mechanics.[3,4] In all of them nominal values of the orbital parameters, velocity increments, and angular values of the plane changes required by a given transfer mission appear in the expressions defining their elements.

An application of this method to a typical shuttle-based transfer mission with 20 deg plane change was described in Ref. 5. The present paper includes an application to a single-stage coplanar transfer from a suborbital ascent trajectory into a Sun-synchronous orbit, using a booster-initialized spin-stabilized stage vehicle with a time-constrained apogee motor.

Description of the Method

The general case of a two-impulse noncoplanar orbital transfer is analyzed. Time-constrained impulses are applied near the extremes of the transfer orbit. The algorithm illustrated in Fig. 1 is described in the following paragraphs.

Presented as Paper 79-0256 at the 17th Aerospace Sciences Meeting, New Orleans, La., Jan. 15-17, 1979; submitted Jan. 31, 1979; revision received Aug. 8, 1979.

Index categories: LV/M Trajectories and Tracking Systems; LV/M Dynamics and Control; Earth Orbital Trajectories.

*Section Chief, Spacecraft R&D; formerly Mgr., Dynamics & Control, Fairchild Space & Electronics Co. Member AIAA.

†Principal Systems Design Engineer.

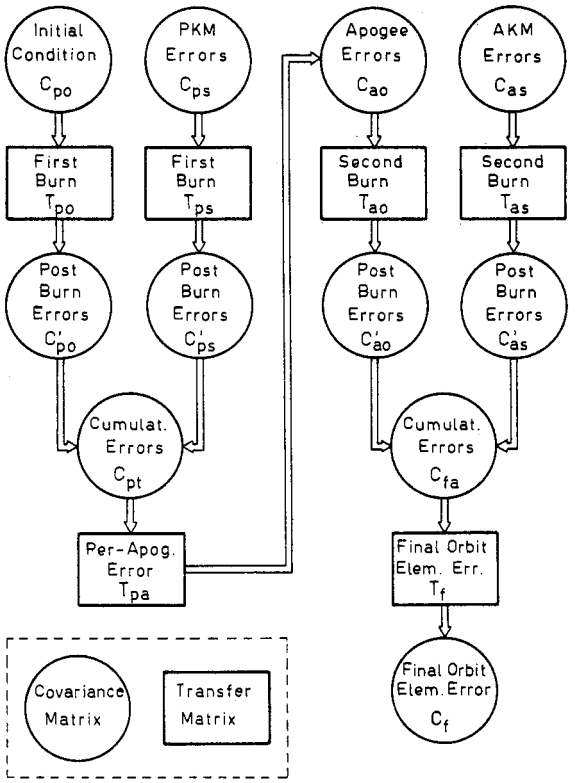

Fig. 1 Illustration of algorithm.

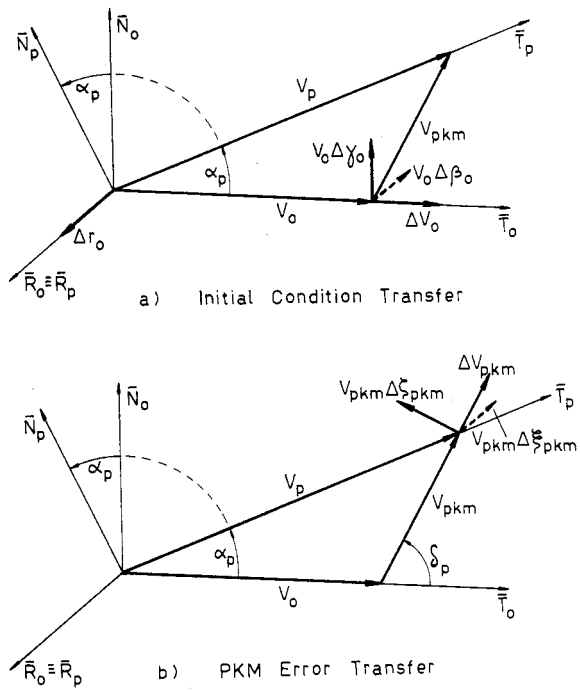

Fig. 2 Transfer through first burn.

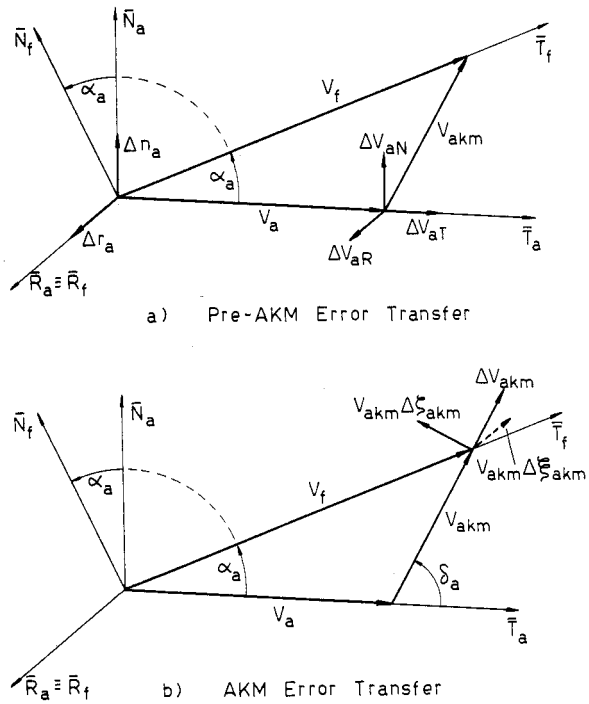

Fig. 3 Transfer through second burn.

Input Errors

1) C_{p0} is the covariance matrix of the initial condition errors Δr_0, ΔV_0, $\Delta\beta_0$, and $\Delta\gamma_0$. For a conventional launch vehicle, this matrix is normally generated by the launch vehicle supplier; for a shuttle mission, this matrix describes the stage vehicle error state at the time of first motor ignition.

2) C_{ps} and C_{as} are the covariance matrices of the impulse (ΔV), attitude ($\Delta\xi$,$\Delta\zeta$), and timing (Δt) errors contributed by the perigee kick motor (PKM) and the apogee kick motor (AKM).

The impulse error depends upon the motor selection. The attitude errors during burn depend on the stage vehicle mode of operation after separation from the launch vehicle, i.e., on whether the stage vehicle is spin stabilized or body stabilized during burn. They are additionally dependent upon whether the stage vehicle attitude throughout the orbital transfer is tied to the original attitude established by the launch vehicle prior to separation, or is initialized prior to each burn by an attitude control system. These options, available to the stage vehicle/spacecraft system designer, are important tradeoff elements in evaluating the system cost/complexity vs orbit insertion accuracy. However, they exceed the scope and limitations of this paper. Suffice it to say that a preliminary dynamic analysis of the stage/space vehicle system throughout the orbital transfer is necessary to assess the expected attitude/nutation errors during each burn.

The Algorithm

1) The matrix C_{p0} (set Δr_0, ΔV_0, $\Delta\beta_0$, $\Delta\gamma_0$), expressed in the orthogonal right-handed orbital coordinates R_0, T_0, N_0 (outward radial, forward tangential, normal), is transformed by the transfer matrix T_{p0} into an equivalent matrix C'_{p0} (set Δr_p, ΔV_p, $\Delta\beta_p$, $\Delta\gamma_p$), expressed in post-burn coordinates R_p, T_p, N_p (Fig. 2a):

$$C'_{p0} = T_{p0} C_{p0} T'_{p0} \tag{1}$$

2) The matrix C_{ps} (set ΔV_{PKM}, $\Delta\xi_{\mathrm{PKM}}$, $\Delta\zeta_{\mathrm{PKM}}$, Δt_{PKM}), expressed in body axes, is similarly transformed into an equivalent matrix C'_{ps} in the set Δr_p, ΔV_p, $\Delta\beta_p$, $\Delta\gamma_p$ (Fig. 2b):

$$C'_{ps} = T_{ps} C_{ps} T'_{ps} \tag{2}$$

3) The covariance matrices C'_{p0} and C'_{ps} can be added to describe the vehicle error state at the end of first burn (begin of transfer orbit):

$$C_{pt} = C'_{p0} + C'_{ps} \tag{3}$$

4) The matrix C_{pt} (set Δr_p, ΔV_p, $\Delta\beta_p$, $\Delta\gamma_p$) is then transformed into the matrix C_{a0} (covariance matrix of the "initial" condition prior to second burn) in the set Δr_a, Δn_a, ΔV_{aR}, ΔV_{aT}, ΔV_{aN}. The tangential position error is not

relevant to this analysis and is omitted. The transfer equation is

$$C_{a0} = T_{pa} C_{pt} T'_{pa} \tag{4}$$

5) As before, C_{a0} and the AKM error covariance matrix C_{as} are transformed (Fig. 3) into equivalent post-burn matrices C'_{a0}, C'_{as} (set Δr_f, Δn_f, ΔV_{fR}, ΔV_{fT}, ΔV_{fN}):

$$C'_{a0} = T_{a0} C_{a0} T'_{a0} \tag{5}$$

$$C'_{as} = T_{as} C_{as} T'_{as} \tag{6}$$

and are added to describe the vehicle error state at the end of second burn (begin of final orbit):

$$C_{fa} = C'_{a0} + C'_{as} \tag{7}$$

6) A final transformation T_f transforms C_{fa} into the covariance matrix C_{fe} of the final orbit element errors (Δa_f, Δe_f, Δi_f, $\Delta\Omega_f$):

$$C_f = T_f C_{fa} T'_f \tag{8}$$

The following special cases can be analyzed:

1) Coplanar two-impulse Hohman transfer. Set equal to zero the value of the plane change in the transformation matrices of Eqs. (1) and (2), or (5) and (6), or both.

2) Single- or tandem-stage perigee or apogee insertion. Set equal to zero the appropriate stage error covariance matrix and the apogee or perigee plane change, where required.

Note that, although the general formulation of the method implies a first burn at perigee, the algorithm is applicable to apogee insertion missions from ballistic ascent trajectories. To this purpose, the matrix T_{pa} has been developed with the capability of accepting any begin-of-transfer anomaly ($\phi_p \neq 0$).

The Transfer Matrices

Definition: Let the transfer matrix T_{ab} transform the m-dimensional error set A into the n-dimensional error set B. The (i,j) element of the matrix is defined by $T_{ab}(i,j) = \partial B_i / \partial A_j$.

Initial Condition Errors Through First Burn Transfer Matrix, T_{p0}

The matrix T_{p0}, for the transformation of Δr_0, ΔV_0, $\Delta\beta_0$, $\Delta\gamma_0$ into Δr_p, ΔV_p, $\Delta\beta_p$, $\Delta\gamma_p$, is defined by:

$$\begin{bmatrix} \Delta r_p \\ V_p \\ \Delta\beta_p \\ \Delta\gamma_p \end{bmatrix} = \begin{bmatrix} 1 & 0 & 0 & 0 \\ 0 & \alpha & 0 & V_0 s\alpha_p \\ 0 & 0 & V_0/V_p & 0 \\ 0 & -(1/V_p) s\alpha_p & 0 & (V_0/V_p) c\alpha_p \end{bmatrix} \begin{bmatrix} \Delta r_0 \\ \Delta V_0 \\ \Delta\beta_0 \\ \Delta\gamma_0 \end{bmatrix} \tag{9}$$

PKM Errors Through First Burn Transfer Matrix, T_{ps}

The matrix T_{ps}, which transforms ΔV_{PKM}, $\Delta\xi_{\mathrm{PKM}}$, $\Delta\zeta_{\mathrm{PKM}}$, Δt_{PKM}, into Δr_p, ΔV_p, $\Delta\beta_p$, $\Delta\gamma_p$ is defined by Eq. (10). The element T_{ps} (3,4) (row 3, column 4) is derived in Appendix B, Eq. (B3).

$$\begin{bmatrix} \Delta r_p \\ \Delta V_p \\ \Delta\beta_p \\ \Delta\gamma_p \end{bmatrix} = \begin{bmatrix} 0 & 0 & 0 & 0 \\ c(\delta_p - \alpha_p) & 0 & -V_{\mathrm{PKM}} s(\delta_p - \alpha_p) & 0 \\ 0 & \dfrac{V_{\mathrm{PKM}}}{V_p} & 0 & \dfrac{V_0}{r_p}\left[c\alpha_p - \dfrac{V_0}{V_p(1-e_0)}\right] \\ \dfrac{s(\delta_p - \alpha_p)}{V_p} & 0 & \dfrac{V_{\mathrm{PKM}} c(\delta_p - \alpha_p)}{V_p} & 0 \end{bmatrix} \begin{bmatrix} \Delta V_{\mathrm{PKM}} \\ \Delta\xi_{\mathrm{PKM}} \\ \Delta\zeta_{\mathrm{PKM}} \\ \Delta t_{\mathrm{PKM}} \end{bmatrix} \tag{10}$$

Table 1 Transfer matrix T_{pa}

	Δr_p	ΔV_p	$\Delta\beta_p$	$\Delta\gamma_p$
Δr_a	$\dfrac{(1+ec\phi_p)(2-e+c\phi_p)}{(1-e)^2}$	$\dfrac{2a(1+e)(1+c\phi_p)}{V_p(1-e)}$	$-\dfrac{a(1-e^2)s\phi_p}{1+ec\phi_p}$	0
Δn_a	0	0	0	$r_a s\phi_p$
ΔV_{aR}	$\left(\dfrac{\partial V_{aR}}{\partial\phi_a}\right)\left(\dfrac{\partial\phi_a}{\partial E_a}\right)\left(\dfrac{\partial E_a}{\partial r_p}\right)$	$\left(\dfrac{\partial V_{aR}}{\partial\phi_a}\right)\left(\dfrac{\partial\phi_a}{\partial E_a}\right)\left(\dfrac{\partial E_a}{\partial V_p}\right)$	$\left(\dfrac{\partial V_{aR}}{\partial\phi_a}\right)\left(\dfrac{\partial\phi_a}{\partial E_a}\right)\left(\dfrac{\partial E_a}{\partial\beta_p}\right)$	0
ΔV_{aT}	$-\dfrac{V_a(1+c\phi_p)}{r_p(1-e)}$	$-\dfrac{V_a(1+e+2c\phi_p)}{V_p(1-e)}$	$\dfrac{V_a s\phi_p}{1+ec\phi_p}$	0
ΔV_{aN}	0	0	0	$-V_a c\phi_p$

Transfer Matrix, T_{pa}

The matrix T_{pa} which propagates C_{pt} (set Δr_p, ΔV_p, $\Delta\beta_p$, $\Delta\gamma_p$) into C_{a0} (set Δr_a, Δn_a, ΔV_{aR}, ΔV_{aT}, ΔV_{aN}) is defined in Table 1. Its derivation is described in Appendix A.

An earlier method of error propagation along a conical coast arc, with no restriction on the position of the end points, is described in Ref. 6. Its main differences from this approach are: 1) It does not include the effects of a launch vehicle-initialized, spin-stabilized stage with a time-constrained AKM on the propagation of Δr_p, ΔV_p, and $\Delta\beta_p$ into the near-apogee radial velocity error. 2) It does not provide closed-form solutions.

Apogee Errors Through Second Burn Transfer Matrix, T_{a0}

The matrix T_{a0}, which transforms C_{a0} into C'_{a0} (set Δr_f, Δn_f, ΔV_{fR}, ΔV_{fT}, ΔV_{fN}), is defined by:

$$\begin{bmatrix} \Delta r_f \\ \Delta n_f \\ \Delta V_{fR} \\ \Delta V_{fT} \\ \Delta V_{fN} \end{bmatrix} = \begin{bmatrix} 1 & 0 & 0 & 0 & 0 \\ 0 & c\alpha_a & 0 & 0 & 0 \\ 0 & 0 & 1 & 0 & 0 \\ 0 & 0 & 0 & c\alpha_a & s\alpha_a \\ 0 & 0 & 0 & -s\alpha_a & c\alpha_a \end{bmatrix} \begin{bmatrix} \Delta r_a \\ \Delta n_a \\ \Delta V_{aR} \\ \Delta V_{aT} \\ \Delta V_{aN} \end{bmatrix} \tag{11}$$

AKM Errors Through Second Burn Transfer Matrix, T_{as}

The matrix T_{as}, which transforms the AKM errors ΔV_{AKM}, $\Delta\xi_{\mathrm{AKM}}$, $\Delta\zeta_{\mathrm{AKM}}$, Δt_{AKM} into Δr_f, Δn_f, ΔV_{fR}, ΔV_{fT}, ΔV_{fN}, is defined by:

$$\begin{bmatrix} \Delta r_f \\ \Delta n_f \\ \Delta V_{fR} \\ \Delta V_{fT} \\ \Delta V_{fN} \end{bmatrix} = \begin{bmatrix} 0 & 0 & 0 & 0 \\ 0 & 0 & 0 & 0 \\ 0 & -V_{\mathrm{AKM}} & 0 & \frac{V_a}{r_a}\left(V_f c\alpha_a - \frac{V_a}{1-e}\right) \\ c(\delta_a-\alpha_a) & 0 & -V_{\mathrm{AKM}} s(\delta_a-\alpha_a) & 0 \\ s(\delta_a-\alpha_a) & 0 & V_{\mathrm{AKM}} c(\delta_a-\alpha_a) & 0 \end{bmatrix} \begin{bmatrix} \Delta V_{\mathrm{AKM}} \\ \Delta\xi_{\mathrm{AKM}} \\ \Delta\zeta_{\mathrm{AKM}} \\ \Delta t_{\mathrm{AKM}} \end{bmatrix} \tag{12}$$

Table 2 Transfer matrix T_f

	Δr_f	Δn_f	ΔV_{fR}	ΔV_{fT}	ΔV_{fN}
Δa_f	$2(a_f/r_f)^2$	0	0	$\frac{2a_f(2a_f-r_f)}{V_f r_f}$	0
Δe_{f1}	$(e_f+c\phi_f)/r_f$	0	0	$2(e_f+c\phi_f)/V_f$	0
Δe_{f2}	0	0	0 (elliptic orbits) $1/V_f$ (circular orbits)	0	0
Δi_f	0	$s\lambda_a/r_f s i_f$ $1/r_f$ (for $i_f=0$)	0	0	$\frac{\sqrt{s^2 i_f - s^2\lambda_a}}{V_f s i_f}$ $1/V_f$ (for $i_f=0$)
$\Delta\Omega_f$	0	$-\frac{\sqrt{s^2 i_f - s^2\lambda_a}}{r_f s^2 i_f}$ 0 (for $i_f=0$)	0	0	$s\lambda_a/(V_f s^2 i_f)$ 0 (for $i_f=0$)

Table 3 Modified apogee error covariance matrix

	r_f, m	n_f, m	V_{fR}, m/s	V_{fT}, m/s	V_{fN}, m/s
r_f	2,135,000	0	0.07663	−0.5886	0
n_f	0	1,559,000	0	0	0.1359
V_{fR}	1312	0	137.4	−0.03023	0.9574
V_{fT}	−2417	0	−0.9959	7.899	0
V_{fN}	0	1939	128.3	0	130.7
3σ error	4384	3745	35.16	8.43	34.29

Table 4 Modified final orbit error covariance matrix

	a_f, m	e_{f1}	e_{f2}	i_f, deg	Ω_f deg
a_f	17,570,000	0.9454	0.01605	0	0
e_{f1}	2.547	4.1×10^{-7}	−0.009976	0	0
e_{f2}	0.1043	-9.9×10^{-9}	2.4×10^{-6}	−0.9605	−0.8013
i_f	0	0	1.25×10^{-4}	0.0071	−0.8856
Ω_f	0	0	-2.8×10^{-5}	−0.00169	5.15×10^{-4}
3σ error	12,570	0.00193	0.00465	0.2528	0.0681

The element T_{as} (3,4), (row 3, column 4) is derived in Appendix B, Eq. (B2).

Final Orbit Transfer Matrix, T_f

The matrix T_f, which transforms C_{fa} into C_f, is defined in Table 2, and derived in Appendix C.

Example

The following is an application to a single-stage coplanar transfer from a suborbital ascent trajectory, which starts at the booster separation altitude of 260 km, into a 600 km circular Sun-synchronous orbit, using a booster-initialized spin-stabilized stage vehicle with a time-constrained apogee motor.

Nominal Parameters

a	=5,821,992 m	ϕ_p	=142 deg	a_f	=6,970,805 m
e	=0.197323	r_a	=6,970,805 m	e_f	=0
τ	=4421 s	V_a	=6774.85 m/s	i_f	=97.73 deg
r_p	=6,634,039 m	λ_a	=12.44 deg S	ϕ_f	=0 deg
V_p	=7189.62 m/s	V_f	=7561.78 m/s	V_{AKM}	=786.93 m/s

In the absence of a PKM and a plane change, the following additional entries are made:

$$V_0=V_p \quad V_{PKM}=0 \quad e_0=e \quad \alpha_p=\alpha_a=\delta_p=\delta_a=0$$

Expected 3σ Initial Condition Errors

The expected 3σ initial condition errors are:

3σ Errors	Correlation coefficients
Δr_0 =457.2 m	$\Delta r_0-\Delta V_0$ = −0.3
ΔV_0 =3.35 m/s	$\Delta r_0-\Delta\beta_0$ = −0.8
$\Delta\beta_0$ =0.06 deg	$\Delta V_0-\Delta\beta_0$ = +0.4
$\Delta\gamma_0$ =0.05 deg	

Expected 3σ AKM Errors

ΔV_{AKM}	=5.9 m/s (0.75%)
$\Delta\xi_{AKM}=\Delta\zeta_{AKM}$	=2.47 deg
Δt_{AKM}	=10 s

The above data determine the initial condition and the AKM error covariance matrices. The relevant transfer matrices are obtained from the nominal parameters. Due to the absence of PKM and plane change, the matrix T_{ps} is irrelevant and T_{p0} and T_{a0} are unity. The "modified" post-burn and final orbit element error matrices are given in Tables 3 and 4. The modification indicates replacement of the matrix elements above the main diagonal with the corresponding correlation coefficients. These tables also show the 3σ errors.

Conclusions

An algorithm for closed-form propagation and estimation of the orbit insertion errors in two-impulse noncoplanar orbital transfers, with time-constrained impulses, has been presented. By skillful use, the flexibility of the algorithm makes it applicable to most shuttle-based transfer missions, as well as missions originated by conventional launchers.

Appendix A: Derivation of Transfer Matrix T_{pa}

For generality, it is assumed that the transfer is non-Hohman, with the transfer angle to nominal apogee less than 180 deg. The approach consists of: 1) determining the effects of the initial point errors (Δr_p, ΔV_p, $\Delta\beta_p$, $\Delta\gamma_p$) on the transfer orbit elements a, e, τ; 2) determining the effects of these and of the initial point errors on the near-apogee altitude, transverse displacement, and velocity error components.

Effects of Δr_p

Effects on Transfer Orbit Elements

1) Effects on semi-major axis: From

$$V^2/\mu+1/a=2r \tag{A1}$$

differentiation at the initial point, with $V=V_p=$const. yields

$$\partial a/\partial r_p=2(a/r_p)^2=2\{r_a/[r_p(1+e)]\}^2 \tag{A2}$$

2) Effect on period: From $\tau=2\pi\sqrt{a^3/\mu}$

$$\partial\tau/\partial r_p=(\partial\tau/\partial r_a)(\partial r_a/\partial r_p)=3\tau a/r_p^2 \tag{A3}$$

3) Effect on eccentricity: From

$$e=\sqrt{1-(V^2r/\mu)(2-V^2r/\mu)s^2\beta} \tag{A4}$$

differentiating with respect to r_p, with $V=V_p=$const., $\beta=\beta_p=$const., and using Eqs. (A1), (A4), and the equation

$$r=a(1-e^2)/(1+ec\phi) \tag{A5}$$

one obtains

$$\partial e/\partial r_p=(e+c\phi_p)/r_p \tag{A6}$$

Effects on Near-Apogee Position and Velocity

1) Effect on radius: From

$$r_a=a(1+e) \tag{A7}$$

by differentiation and use of Eqs. (A2), (A5), and (A6),

$$\partial r_a/\partial r_p=(1+ec\phi_p)(2+c\phi_p-e)/(1-e)^2 \tag{A8}$$

2) Effect on transverse displacement: $\partial n_a/\partial r_p=0$.

3) Effect on tangential velocity component: From Eq. (A1), differentiating at apogee with $V=V_{aT}$ and $r=r_a$, and substituting Eqs. (A1), (A2), (A5) and (A8)

$$\partial V_{aT}/\partial r_p=-(V_a/r_p)(1+c\phi_p)/(1-e) \tag{A9}$$

4) Effect on radial velocity component:

a) Effect on initial condition of eccentric anomaly: From

$$E_p=c^{-1}[(1-r_p/a)/e] \tag{A10}$$

by differentiation and use of Eqs. (A2), (A5), (A6), and of the equation

$$sE = rs\phi/(a\sqrt{1-e^2}) \tag{A11}$$

one obtains

$$\partial E_p/\partial r_p = -a(sE_p/e)/r_p^2$$
$$\partial E_p/\partial r_p = 0 \quad \text{for} \quad e=0 \tag{A12}$$

b) Effect on eccentric anomaly at AKM burn: It is assumed that the AKM is controlled by a timer. Due to variation of the orbital period, under nominal timing conditions the AKM will be ignited before or after true apogee. Let the true and the eccentric anomaly at AKM burn (assumed impulsive) be

$$\phi_a = \pi + \Delta\phi_a \qquad E_a = \pi + \Delta E_a \tag{A13}$$

Since the time from perigee is

$$t = (\tau/2\pi)(E - esE) \tag{A14}$$

the time from the initial point is

$$t' = t - t_p = (\tau/2\pi)[(E - esE) - (E_p - esE_p)] \tag{A15}$$

The nominal time of AKM firing is $\tau/2\text{-}t_p$. Substituting this for t' and incrementing with errors all the variables in Eq. (A15), yields

$$\tau/2 - t_p = [(\tau+\Delta\tau)/2\pi]\{[\pi + \Delta E_a - (e+\Delta e)s(\pi+\Delta E_a)]$$
$$- [E_p + \Delta E_p - (e+\Delta e)s(E_p+\Delta E_p)]\}$$

Simplifying and retaining only first-order terms,

$$\frac{\partial E_a}{\partial r_p} = -\left(\frac{\pi - E_p + esE_p}{\tau(1+e)}\right)\frac{\partial \tau}{\partial r_p} + \left(\frac{1-ecE_p}{1+e}\right)\frac{\partial E_p}{\partial r_p}$$
$$-\left(\frac{sE_p}{1+e}\right)\frac{\partial e}{\partial r_p} \tag{A16}$$

c) Effect on true anomaly at AKM burn: From

$$c\phi = (cE - e)/(1 - ecE) \tag{A17}$$

differentiating with respect to E, yields

$$s\phi\,d\phi = \{[(1-e^2)sE]/(1-ecE)^2\}dE$$

By substitution of Eq. (A13) for the AKM burn conditions and by first-order approximation:

$$\partial\phi_a/\partial E_a = \sqrt{(1-e)/(1+e)} \tag{A18}$$

d) Effect on radial velocity component: From

$$r = p/(1+ec\phi) \quad \text{and} \quad H = r^2\dot{\phi} = \sqrt{\mu p} \tag{A19}$$

by time differentiation, with p and e constant

$$\dot{r} = (\partial r/\partial\phi)\dot{\phi} = (e\mu/H)s\phi = [eV_a/(1-e)]s\phi \tag{A20}$$

Substituting the AKM burn condition [Eq. (A13)] and first-order approximation yield

$$\dot{r} = \Delta\dot{r} = -[eV_a/(1-e)]\Delta\phi_a \tag{A21}$$

The component of radial velocity ΔV_{aR} can be obtained by inspection of Figs. 3 and A1. Since the AKM thrust is nominally orthogonal to the apsidal line, the resultant radial velocity component is

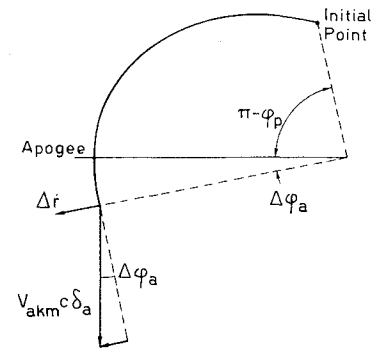

Fig. A1 Relationship between true anomaly and radial velocity.

$$\Delta V_{aR} = \Delta\dot{r} + V_{\mathrm{AKM}}c\delta_a s(\Delta\phi_a)$$

Substituting Eq. (A21), the relationship $V_{\mathrm{AKM}}c\delta_a = V_f c\alpha_a - V_a$ and using first-order approximation

$$\partial V_{aR}/\partial\phi_a = V_f c\alpha_a - V_a/(1-e) \tag{A22}$$

e) Overall effects: The effect of Δr_p on ΔV_{aR}, including the effect of the nominal AKM velocity increment, is

$$(\partial V_{aR}/\partial r_p) = (\partial V_{aR}/\partial\phi_a)(\partial\phi_a/\partial E_a)(\partial E_a/\partial r_p) \tag{A23}$$

If the AKM ignition is independently controlled, $\partial V_{aR}/\partial r_p = 0$.

5) Effect on normal velocity component: The effect is $\partial V_{aN}/\partial r_p = 0$.

Effects of ΔV_p

Effects on Transfer Orbit Elements

1) Effect on semi-major axis: Differentiating Eq. (A1) at the initial point, with $r = r_p = \text{const.}$ yields

$$\partial a/\partial V_p = 2a(2a - r_p)/(r_p V_p) \tag{A24}$$

2) Effect on period: From Eqs (A3) and (A24)

$$\partial\tau/\partial V_p = (\partial\tau/\partial a)(\partial a/\partial V_p) = 3\tau(2a - r_p)/(r_p V_p) \tag{A25}$$

3) Effect on eccentricity: Differentiating Eq. (A4) at the initial point, with $r = r_p = \text{const.}$ and using Eqs. (A1) and (A5)

$$\partial e/\partial V_p = 2(e + c\phi_p)/V_p \tag{A26}$$

Effects on Near-Apogee Position and Velocity

1) Effect on radius: Differentiating Eq. (A7) and substituting Eqs. (A24), (A26), and (A5) yields

$$\partial r_a/\partial V_p = 2a(1 + c\phi_p)(1+e)/[V_p(1-e)] \tag{A27}$$

2) Effect on transverse displacement: $\partial n_a/\partial V_p = 0$.

3) Effect on tangential velocity component: From Eq. (A1), differentiating at apogee with $V = V_{aT}$ and $r = r_a$ and substituting Eqs. (A1), (A5), (A24), and (A27) yields

$$\partial V_{aT}/\partial V_p = -V_a(1 + e + 2c\phi_p)/[V_p(1-e)] \tag{A28}$$

4) Effect on radial velocity component:

a) Effect on initial condition of eccentric anomaly: Differentiating Eq. (A10), and substituting $dr_p = 0$ and Eqs. (A24), (A26), (A5), and (A11),

$$\partial E_p/\partial V_p = -2s\phi_p/(eV_p\sqrt{1-e^2})$$
$$\partial E_p/\partial V_p = 0 \quad \text{for} \quad e=0 \tag{A29}$$

b) Effect on eccentric anomaly at AKM burn: Following the same approach leading to Eq. (A16),

$$\frac{\partial E_a}{\partial V_p} = -\left(\frac{\pi - E_p + esE_p}{\tau(1+e)}\right)\frac{\partial \tau}{\partial V_p} + \left(\frac{1-ecE_p}{1+e}\right)\frac{\partial E_p}{\partial V_p} - \left(\frac{sE_p}{1+e}\right)\frac{\partial e}{\partial V_p} \tag{A30}$$

c) Overall effects: The comprehensive effect, including the effect of the nominal AKM velocity increment, is

$$\partial V_{aR}/\partial V_p = (\partial V_{aR}/\partial \phi_a)(\partial \phi_a/\partial E_a)(\partial E_a/\partial V_p) \tag{A31}$$

If the AKM ignition is independently controlled, $\partial V_{aR}/\partial V_p = 0$.

5) Effect on normal velocity component: $\partial V_{aN}/\partial V_p = 0$.

Effects of $\Delta\beta_p$

Effects on Transfer Orbit Elements

1) Effects on semi-major axis: Differentiating Eq. (A1) with $V = V_p = \text{const.}$ and $r = r_p = \text{const.}$, yields

$$\partial a/\partial \beta_p = 0 \tag{A32}$$

2) Effect on period: From Eq. (A3),

$$\partial \tau/\partial \beta_p = 0 \tag{A33}$$

3) Effect on eccentricity: Differentiating Eq. (A4) at the initial point, with $V = V_p = \text{const.}$ and $r = r_p = \text{const.}$, using Eqs. (A4) and (A5) yields

$$\partial e/\partial \beta_p = -(1-e^2)s\phi_p/(1+ec\phi_p) \tag{A34}$$

Effects on Near-Apogee Position and Velocity

1) Effect on radius: Differentiating Eq. (A7) and substituting Eqs. (A32) and (A34),

$$\partial r_a/\partial \beta_p = -a(1-e^2)s\phi_p/(1+ec\phi_p) \tag{A35}$$

2) Effect on transverse displacement: $\partial n_a/\partial \beta_p = 0$.

3) Effect on tangential velocity component: Differentiating Eq. (A1) at apogee, and substituting Eqs. (A32) and (A35)

$$\partial V_{aT}/\partial \beta_p = V_a s\phi_p/(1+ec\phi_p) \tag{A36}$$

4) Effect on radial velocity component:

a) Effect on initial condition of eccentric anomaly: Differentiating Eq. (A10) and substituting $dr_p = 0$ and Eqs. (A32), (A34), (A5), and (A11) yields

$$\partial E_p/\partial \beta_p = -(e+c\phi_p)\sqrt{1-e^2}/[e(1+ec\phi_p)] \tag{A37}$$

b) Effect on eccentric anomaly at AKM burn: Similar to Eq. (A16)

$$\frac{\partial E_a}{\partial \beta_p} = \left(\frac{1-ecE_p}{1+e}\right)\frac{\partial E_p}{\partial \beta_p} - \left(\frac{sE_p}{1+e}\right)\frac{\partial e}{\partial \beta_p} \tag{A38}$$

c) Overall effects: The comprehensive effect is

$$\partial V_{aR}/\partial \beta_p = (\partial V_{aR}/\partial \phi_a)(\partial \phi_a/\partial E_a)(\partial E_a/\partial \beta_p) \tag{A39}$$

If the AKM ignition is independently controlled, $\partial V_{aR}/\partial \beta_p = 0$.

5) Effect on normal velocity component: $\partial V_{aN}/\partial \beta_p = 0$.

Effects of $\Delta\gamma_p$

An azimuth error $\Delta\gamma_p$ produces a transverse displacement Δn_a of the apogee location and a normal velocity component ΔV_{aN}. Their magnitude is a function of the transfer angle $\pi - \phi_p$. From simple geometrical considerations:

$$\partial n_a/\partial \gamma_p = r_a s\phi_p \tag{A40}$$

$$\partial V_{aN}/\partial \gamma_p = -V_a c\phi_p \tag{A41}$$

Singular Case of Circular Transfer Orbits

The limit case of a circular transfer ($e = 0$) occurs when a two-point burn is used only to change the plane of a circular orbit. The true and the eccentric anomaly at the initial point is typically 0. Note, however, that of the three in-plane source errors Δr_p, ΔV_p, $\Delta\beta_p$ only the effects of the first two are amenable to the limit case evaluation with $e = 0$ and $\phi_p = E_p = 0$. This is because these errors do not modify the orientation of the apsidal line. Thus an apsis arises at the second impulse point, and the expressions derived in the previous sections, seeking the error propagation at that point, yield the correct results. This is not so for $\Delta\beta_p$ which rotates the apsidal line by 90 deg. Modifying Eqs. (A34) and (A38) by using $\phi_p = E_p = 90$ or 270 deg, when $e = 0$, to account for an apsidal line transverse to the nominal impulse line, would yield the correct results at the true apsis, but not at the second impulse point where they are needed. These, however, are still obtained by $\phi_p = E_p = 0$ in Eqs. (A35) and (A36), while Eq. (A39) must be replaced by $\partial V_{aR}/\partial \beta_p = V_p$ of immediate geometrical derivation.

Appendix B: Effects of AKM Timing Error Δt_{AKM}

A timing error Δt_{AKM} causes the AKM to burn at the time $\tau/2 - t_p + \Delta t_{\text{AKM}}$ from the initial point. The true and eccentric anomalies at the burn point are given by Eq. (A13). Substitution into Eq. (A15) yields

$$\partial E_a/\partial t_{\text{AKM}} = 2\pi/[\tau(1+e)] \tag{B1}$$

The effect of Δt_{AKM} on ΔV_{aR}, which is the only first-order effect, can be computed by

$$\partial V_{aR}/\partial t_{\text{AKM}} = (\partial V_{aR}/\partial \phi_a)(\partial \phi_a/\partial E_a)(\partial E_a/\partial t_{\text{AKM}})$$

which, by substitution of Eqs. (A22), (A18), and (B1), and $\tau = 2\pi\sqrt{a^3/\mu}$ yields

$$\partial V_{fR}/\partial t_{\text{AKM}} = \partial V_{aR}/\partial t_{\text{AKM}} = V_a[V_f c\alpha_a - V_a/(1-e)]/r_a \tag{B2}$$

By appropriate change of symbols and by observing that $\Delta\beta_p = \Delta V_{pR}/V_p$, this expression yields the post-perigee burn effect of a PKM timing error on path angle, i.e.,

$$\partial \beta_p/\partial t_{\text{PKM}} = V_0\{c\alpha_p - V_0/[V_p(1-e_0)]\}r_p \tag{B3}$$

Appendix C: Derivation of the Transfer Matrix T_f

Let the nominal parameters of the final orbit be a_f, e_f, i_f, Ω_f. Source errors for this phase are Δr_f, Δn_f, ΔV_{fR}, ΔV_{fT}, ΔV_{fN}, i.e., the insertion point errors.

Effects of Δr_f

The primary effects of Δr_f are semi-major axis and apsidal component of eccentricity variations.

Effects on semi-major axis: From Eq. (A2)

$$\partial a_f/\partial r_f = 2(a_f/r_f)^2 \tag{C1}$$

Effect on eccentricity (apsidal component): From Eq. (A6)

$$\partial e_{fl}/\partial r_f = (e_f + c\phi_f)/r_f \tag{C2}$$

where ϕ_f is the nominal anomaly of the final orbit at the insertion point.

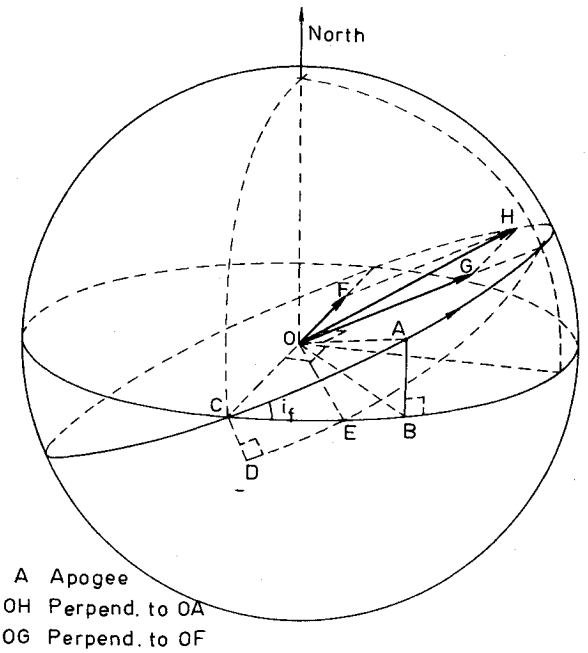

Fig. C1 Effects of Δn_f.

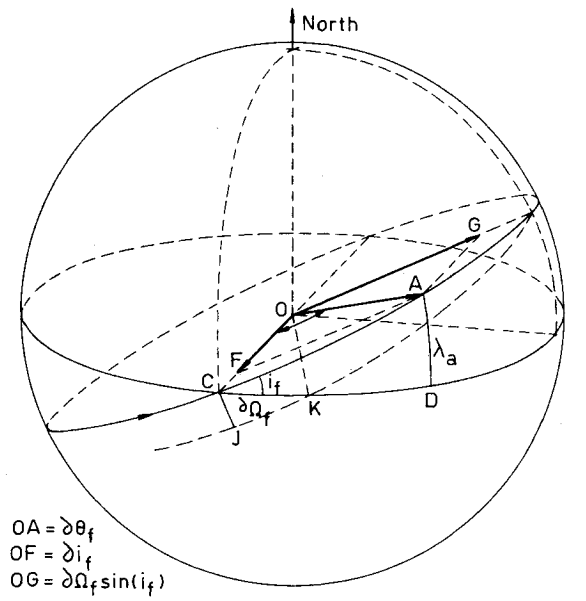

Fig. C2 Effects of ΔV_{fN}.

Effects of Δn_f

A transverse displacement Δn_f corresponds to a rotation $\Delta\psi_f = \Delta n_f / r_f$ of the orbit plane about the radius vector perpendicular to that at apogee. Let this rotation, represented by the vector **OH** in Fig. C1, be decomposed into:

1) Component along the line of nodes, $\mathbf{OF} = \Delta\psi_f s(\mathrm{AC})$.

2) Component perpendicular to the line of nodes, $\mathbf{OG} = \Delta\psi_f c(\mathrm{AC})$. The first component yields an inclination variation. The second, from the triangle CDE, yields the nodal drift $\Delta\Omega_f = (\mathrm{CD}) s i_f = |\mathbf{OG}| / s i_f$. Since

$$s(\mathrm{AC}) = s\lambda_a / s i_f \tag{C3}$$

the above relationships yield

$$\partial i_f / \partial n_f = s\lambda_a / (r_f s i_f)$$

$$\partial\Omega_f / \partial n_f = -(\sqrt{s^2 i_f - s^2\lambda_a}) / (r_f s^2 i_f) \tag{C4}$$

When $i_f = 0$, any rotation $\Delta\psi_f$ affects the nominal inclination, and a nominal nodal position cannot be defined, thus

$$\partial i_f / \partial n_f = 1 / r_f \qquad \partial\Omega_f / \partial n_f = 0$$

Effects of ΔV_{fR}

A radial velocity error primarily affects the transverse component of eccentricity. However, except for the case of a circular final orbit, this effect is negligible. This can be seen as follows. The path angle associated with ΔV_{fR} is $\Delta\beta_f = -\Delta V_{fR} / V_f$, thus from Eq. (A32):

$$\partial a_f / \partial V_{fR} = -(1/V_f)(\partial a_f / \partial\beta_f) = 0 \tag{C5}$$

and from Eq. (A34),

$$\partial e_f / \partial V_{fR} = -(1/V_f)(\partial e_f / \partial\beta_f)$$

$$= [(1 - e_f^2) s\phi_f] / [V_f (1 + e_f c\phi_f)] \tag{C6}$$

For final orbit insertion at perigee or apogee, the nominal value of ϕ_f is respectively 0 or π, which produces $\partial e_f / \partial V_{fR} = 0$. However, for circular orbit insertions, a transverse ovalization arises from ΔV_{fR}, which in the limit implies $\phi_f = \pi/2$, and, from Eq. (C6):

$$\partial e_{f2} / \partial V_{fR} = 1 / V_f \tag{C7}$$

Effects of ΔV_{fT}

As with Δr_f, ΔV_{fT} affects only Δa_f and Δe_{f1}.

Effect on semi-major axis: From Eq. (A24)

$$\partial a_f / \partial V_{fT} = 2a_f (2a_f - r_f) / (r_f V_f) \tag{C8}$$

Effect on eccentricity: From Eq. (A26)

$$\partial e_{f1} / \partial V_{fT} = 2(e_f + c\phi_f) / V_f \tag{C9}$$

Effects of ΔV_{fN}

The effect of ΔV_{fN} is a rotation of the orbit plane by the angle $\Delta\theta_f = \Delta V_{fN} / V_f$ about the line of apsides. This rotation, represented by the vector **OA** of Fig. C2, can be decomposed into: 1) component along the line of nodes, and 2) component perpendicular to the line of nodes. As before, the second component produces the nodal rotation $\Delta\Omega_f = \Delta\theta_f s(\mathrm{AC}) / s i_f$, thus substituting from Eq. (C4):

$$\partial i_f / \partial V_{fN} = (\sqrt{s^2 i_f - s^2\lambda_a}) / (V_f s i_f)$$

$$\partial\Omega_f / \partial V_{fN} = s\lambda_a / (V_f s^2 i_f) \tag{C10}$$

Similarly, for $i_f = 0$, $\partial i_f / \partial V_{fN} = 1 / V_f$, and $\partial\Omega_f / \partial V_{fN} = 0$.

Acknowledgments

This work was company sponsored while both authors were with Fairchild Space and Electronics Co.

References

[1] Gelb, A., *Applied Optimal Estimation,* M.I.T. Press, Cambridge, Mass., 1974.

[2] Mehra, R.K., "On-Line Identification of Linear Dynamic Systems, with Application to Kalman Filtering," *IEEE Transactions on Automatic Control,* Vol. AC-16, No. 1, Feb. 1971.

[3] Jensen J., Townsend, G., Kork, J., and Kraft, D., *Design Guide to Orbital Flight,* McGraw Hill Book Co., New York, 1962.

[4] Kaplan, M.H., *Modern Spacecraft Dynamics and Control,* John Wiley and Sons, New York, 1976.

[5] Spencer, T.M., Glickman, R., and Porcelli, G., "Changing Inclination for Shuttle Payloads," Paper 77-218 presented at XXVIII IAF Congress, Prague, Czechoslovakia, Oct. 1977.

[6] Goodyear, W.H., "A General Method for the Computation of Cartesian Coordinates and Partial Derivatives of the Two-Body Problem," NASA CR-522, Sept. 1966.